

## MICROBIAL MEDIATED SYNTHESIS OF GOLD NANOPARTICLES: PREPARATION, CHARACTERIZATION AND CYTOTOXICITY STUDIES

IRENA MALISZEWSKA\*

*Division of Medicinal Chemistry and Microbiology, Faculty of Chemistry,  
Wroclaw University of Technology, 50-370 Wroclaw, Wybrzeże Wyspiańskiego  
27, POLAND*

The present contribution focuses on the synthesis of metallic nanoparticles of gold using aqueous Au<sup>3+</sup> ions with the cell-free filtrate of *Trichoderma koningii*. Fourier transform infrared spectroscopy (FTIR spectrum) suggested that proteins are mainly responsible for reduction of gold ions and long-term stability of the biogenic nanoparticles. The sucrose density gradient technique to separate the gold nanoparticles based on their size was demonstrated. The smallest spheres from 10 nm to 14 nm were concentrated in the 30% fraction and their cytotoxicity was studied. The results suggested that the gold nanoparticles were taken up by the colon cancer cells via endocytosis and the filtrate protein is responsible for their noticeable toxicity against human cancer LoVo and LoVo/DX cells.

(Received June 16, 2013; Accepted August 20, 2013)

*Keywords:* biosynthesis, molds, gold nanoparticles, cytotoxicity, endocytosis

### 1. Introduction

Nanoscale metal materials have been exponentially developed in recent years because of their unique chemical and physical properties and important applications in chemical sensing, biolabeling, diagnostics and therapeutics [1, 2]. Owing to the wide range of applications offered by metal nanoparticles in different fields of science and technology, various protocols have been designed for their formation [3-4]. One of the approaches is the facile synthesis carried out by microorganisms. In the past three decades, it has been shown that several types of bacteria, yeast and fungi had a high ability to synthesize various metallic nanoparticles [5-6]. Among them, molds have been documented as an extremely good candidate in the synthesis of these nanoscale materials [7-8]. The capacity for metal nanoparticles formation was detected in *Verticillium luteoalbum* [9], *Fusarium oxysporum* [10], *Colletotrichum* sp. and *Tricothecium* sp. [11], *Phaenerochaete* sp. [12], *Trichoderma koningii* [13], *Aspergillus foetidus* [14], *Aspergillus niger* [15, 16], *Penicillium* sp. [17] and *Alternaria alternata* [18].

On the other hand, it is known that practical application of gold nanoparticles depends largely on their impact on human and environment health. Nowadays there is a wider debate about the possible risks associated with gold nanoparticles applications. During recent years different studies have been performed demonstrating that nanomaterials can affect biological behaviours at the cellular, subcellular and protein levels. According to Pan et al. [19] studies, smaller size particles have better ability to induce cytotoxicity as compared to bigger one. Moreover, the results obtained suggested that cationic particles are generally toxic at much lower concentrations than anionic particles, which they relate to the electrostatic interaction between the cationic nanoparticles and the negatively charged cell membranes [20]. Cytotoxicity also depends on the type of cells used. For example, 33 nm citrate-capped gold nanospheres were found to be noncytotoxic to baby hamster kidney and human hepatocellular liver carcinoma cells, but cytotoxic to a human carcinoma lung [21].

---

\*Corresponding author: irena.helena.maliszewska@pwr.wroc.pl

In the present study, I used the cell-free filtrate of *Trichoderma koningii* [13] for bio-reduction of the gold ions resulted in extracellular formation of very stable gold nanoparticles. The main aim of this research was to examine *in vitro* toxicity of these biogenic nanostructures on human colon cancer cell line LoVo and multidrug resistance sub-line LoVo/DX. My studies importantly approach to understand the potential toxicity hazards of this biogenic material.

## 2. Materials and methods

### *Reagents*

All chemical agents including chloroauric acid ( $\text{HAuCl}_4 \times 4\text{H}_2\text{O}$ ) were obtained from (POCH) Poland.

### *Synthesis and characterization of the gold nanoparticles*

*Trichoderma koningii* strain, isolated from the soil have been used in the study [13]. The basal medium used in experiments consisted of (%) :  $\text{KH}_2\text{PO}_4$  0.7 ;  $\text{K}_2\text{HPO}_4$  0.2;  $\text{MgSO}_4 \times 7\text{H}_2\text{O}$  0.01;  $\text{NH}_4\text{Cl}$  1.0; yeast extract 0.06; glucose 1.0. The Erlenmeyer flasks were inoculated with spores ( $10^5/\text{mL}$ ) of *Trichoderma koningii* and incubated at  $28^\circ\text{C}$  with shaking (200 rpm) for 5 days. After the fermentation time, the biomass was filtered (Whatman filter paper No. 1) and then extensively washed with distilled water to remove any medium component. Fresh and clean biomass (10 g) was taken into the Erlenmeyer flask, containing 100 mL of Milli-Q deionised water (UV Ultrapure Water System, Burnstead, USA). The flask was agitated at  $28^\circ\text{C}$  with shaking (100 rpm) for 48 h. The cell-free filtrate was collected by pre-filtration in Whatman No. 1 filter papers and filtered using Millex-GP filter (PES membrane,  $0.22\ \mu\text{m}$ ). Chloroauric acid (1 mM of final concentration) was mixed with the cell-free filtrate in an Erlenmeyer flask and agitated at  $28^\circ\text{C}$  in dark. The control (without the cell-free filtrate) was also run along with the experimental flasks. To verify reduction of gold ions the solutions were scanned in the range of 200-800 nm in a spectrophotometer (Shimadzu, UV 3600). The size and morphology of the nanoparticles were analyzed with the transmission electron microscope TEM (Zeiss EM 900). The sample was prepared by placing a drop of the gold nanoparticles on a carbon-coated copper grid and subsequently drying in air before transferring it to the microscope. From electron micrographs the particle size was found for no less than 150 particles.

### *Separation of the gold nanoparticles*

The separation of the gold nanoparticles was performed according to the method described by Kumar et al. [22] with minor modifications. In detail, we created a discontinuous sucrose density gradient by layering dilute sucrose solutions upon one another in a centrifuge tube: 7 mL of 30%, 40%, 50% and 60% w/v sucrose. Finally 7 mL of the gold nanoparticles synthesized by the cell-free filtrate obtained from 5-days biomass cultured in media contained  $\text{NH}_4\text{Cl}$  as nitrogen source with intensive shaking (AuNPs) was loaded onto this gradient and centrifuged at  $2320 \times g$  at  $10^\circ\text{C}$  for 1h. Fractions of the gradient were collected using a pipette, dialyzed (MWCO 8000-10000) against Milli-Q deionised water at room temperature and lyophilized (Freeze Dryer Modulyo, Edwards). These particles were made in a KBr pellet and the spectrum was recorded with FTIR spectrometer (Perkin Elmer 1600). The stability study of the gold nanoparticles was carried out at room temperature. The change in surface plasmon resonance of the nanoparticle dispersion was recorded up to six month using UV-vis spectroscopy. Zeta potential of the gold nanoparticles concentrated in the 30% sucrose fraction (AuNPs-30) was determined using Zetasizer 2000, Malvern Instruments.

### *Assessment of cytotoxic effect*

Human colon adenocarcinoma cell line LoVo and multidrug resistance sub-line LoVo/DX used in our experiments were kindly provided by Joanna Wietrzyk, professor of the Ludwik Hirszfild Institute of Immunology and Experimental Therapy Polish Academy of Science, Wrocław. The studied cancer cells were cultured in OptiMEM+RPMI 1640 medium (1:1) supplement with 5% heat-inactivated foetal bovine serum, 1% of 2 mM L-glutamine and 1% of 1mM sodium pyruvate, 100 IU/ml penicillin and 100  $\mu\text{g}/\text{ml}$  streptomycin.

The effect of the gold particles concentrated in the 30% sucrose fraction on the microscopic morphology of the human cancer cells (LoVo) was studied. A total  $10^5$  cells per well (100  $\mu$ l) were plated in 96-well plates and incubated in 5%  $\text{CO}_2$  at 37 °C for 24 h ( $\text{CO}_2$  – incubator, ASSAB). Then the medium in the wells was replaced with fresh medium containing AuNPs-30 at the concentration of 100  $\mu\text{g}/\text{mL}$ . After 24 hours, the morphological changes of the cells were studied by fluorescence microscopy (Olympus BHS) and transmission electron microscopy. For TEM studies the cells were harvested by scraping and fixed with 2.5% (w/v) glutaraldehyde solution and post fixed in aqueous osmium tetroxide. The sample was then dehydrated in a graded series of ethanol, block stained in uranyl acetate, and embedded in Epon. Ultrathin sections (100 nm) were contrasted with lead citrate and imaged by TEM (Zeiss EM 900).

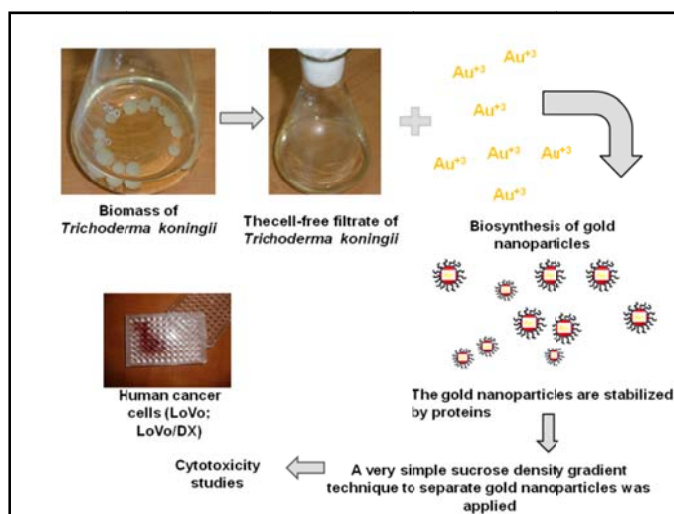
A known amount of lyophilized powders of CF, AuNPs and AuNPs-30 was dispersed in 10 mL of Milli-Q deionised water and filtered using Millex-GP filter (PES membrane, 0.22  $\mu\text{m}$ ). To determine cytotoxic effects, cancer cells (LoVo and LoVo/DX) were subsequently exposed to CF, AuNPs and AuNPs-30 using a concentration range of 1  $\mu\text{g}/\text{mL}$ -1000  $\mu\text{g}/\text{mL}$ . The cells were incubated at 37 °C for 72 h. Cell survival efficiency was measured using SRB assay according to the procedure described by Skehan et al. [23] with a slight modification. For the assay, cells were fixed by layering 50  $\mu$ l of ice-cold 50% trichloroacetic acid (TCA) on top of the growth medium. Cells were incubated at 4 °C for 1 hour, after which plates were washed five times with cold water, excess water drained off and the plates left to dry in air. SRB stain (50  $\mu$ l; 0.4% in 1% acetic acid) was added to each well and allowed to be in contact with the cell for 30 minutes. Subsequently, to remove excess dye, they were washed with 1% acetic acid, rinsed 5 times until only dye adhering to the cells was left. The plates were dried and 150  $\mu$ l of 10 nM Tris (hydroxymethyl)aminomethane (pH 10.5, Sigma) was added to each well to solubilise the dye. The plates were shaken gently for 20 minutes on a gyratory shaker. The absorbance (OD) of each well was read at 492 nm. The percentage of cell survival is expressed as the mean absorbance of the treated cells divided by the mean absorbance of untreated control cells. The 50% inhibitory concentration ( $\text{IC}_{50}$ ) of the gold nanoparticles and the cell-free filtrate was calculated. The data reported represented the means of the triplicate measurements in a separate experiment.

#### *Statistical analysis*

All experiments were run in triplicate and acquired data are expressed as mean  $\pm$ SD.

### **3. Results and discussion**

The strategy applied for size-controlled fabrication and cytotoxicity studies of the biogenic gold nanoparticles is presented in Scheme 1.



*Scheme 1. General concept of our study of gold nanoparticles synthesis by Trichoderma koningii.*

As shown gold ions were reduced during exposure to the *Trichoderma koningii* cell-free filtrate. The nanoparticles formation was visually observed by the color of the reaction mixture changing from colorless to red. A characteristic of all gold colloids is the color which can vary between light red via purple-red to bluish-red [24]. This effect is caused by a surface plasmon resonance (SPR) described by the Mie theory [25]. The appearance of red color in solution containing the cell free filtrate of *Trichoderma koningii* and gold ions suggested the formation of colloidal gold nanoparticles in the medium. According to the Mie theory, spherical gold nanoparticles exhibit only one SPR band, usually in the region of 500-600 nm, whereas anisotropic particles show two or three bands. Figure 1 shows the UV-vis absorption spectrum recorded from the gold nanoparticles solution after 24 h of reaction. The results indicate that the reaction solution has an absorption maximum at about 524 nm attributed to the surface plasmon resonance band of the gold nanoparticles.

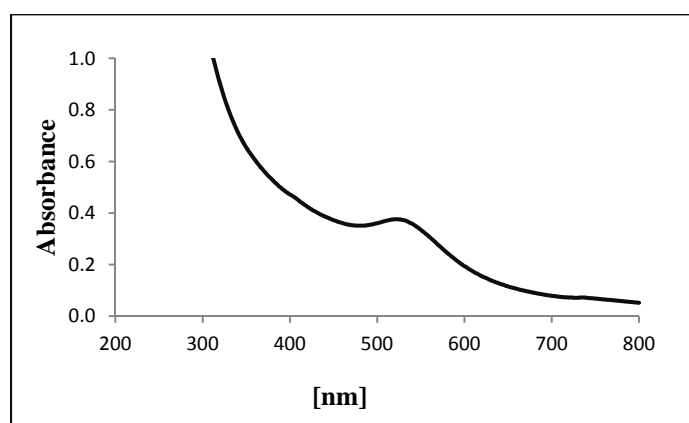


Fig. 1. UV-vis spectrum of the gold nanoparticles synthesized by the cell-free filtrate of *Trichoderma koningii*

For separation of gold particles synthesized the sucrose gradient technique was applied. This method is often used to separate organelles or viruses by ultracentrifugation. It was possible to separate the nanoparticles based on their size by a density gradient of 30% to 70% sucrose using centrifuge with low speeds. Fractions of 3,5 mL were collected and monitored for separation by TEM technique. Figure 2A shows that AuNPs are symmetrical and spherical shaped, well distributed without aggregation in solution with average size is about  $14\pm 4$  nm. Spheres from 10 nm to 14 nm were concentrated in the 30% fraction (Figure 2B) and spheres from 12 nm to 17 nm in the 40% (Figure 2C). Gold nanoparticles have not been observed in fractions 50%-70%.

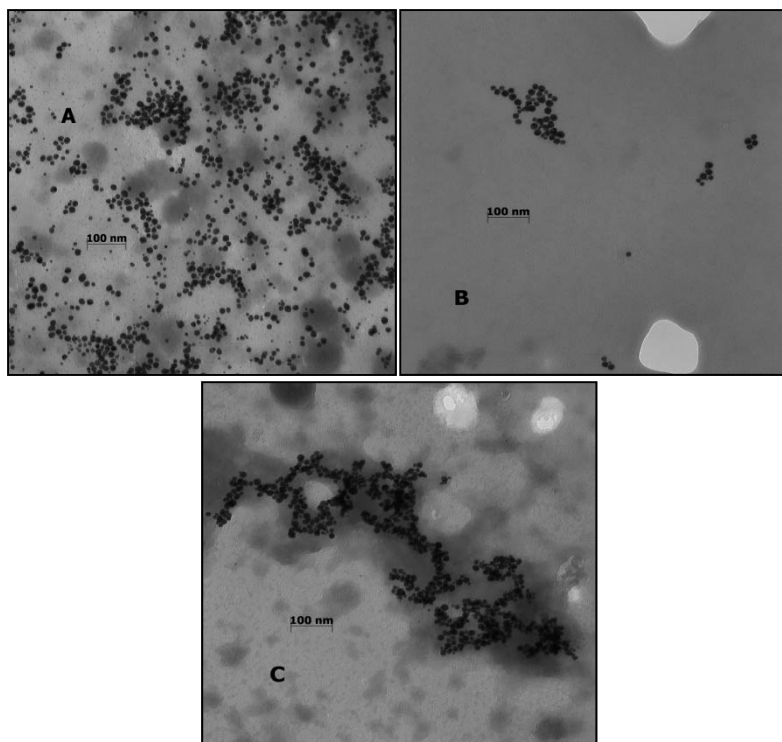


Fig. 2. TEM images of gold nanoparticles synthesized by the cell-free filtrate of *Trichoderma koningii*: (A) before concentration (A); from fraction collected at 30% (B); from fraction collected at 40% (C)

In comparison with other separation protocols such as electrophoresis [26, 27], diafiltration [27], chromatography [29], sucrose density gradient separation is easier to carry out and takes less time.

It is well-known that the practical application of gold nanoparticles significantly depends on their time-dependent stability. To investigate the stability of gold nanostructures, the particles concentrated in the 30% sucrose fraction were stored at room temperature for the period of 6 months. Any precipitation is not observed even after 6 months of storage suggesting that these colloidal gold nanoparticles are extremely stable. Such long-term stability of the particles indicated that nanostructures are stabilized in the solution by the capping agent, which is likely to be protein secreted by *Trichoderma koningii*. FTIR spectroscopy measurements were carried out to identify the molecules that bound specially on the gold surface. Representative spectrum of the obtained nanoparticles shows the presence of absorption peaks located at about  $3410\text{ cm}^{-1}$ ,  $1560\text{ cm}^{-1}$ ,  $1350\text{ cm}^{-1}$  and  $1065\text{ cm}^{-1}$  (Figure 3).

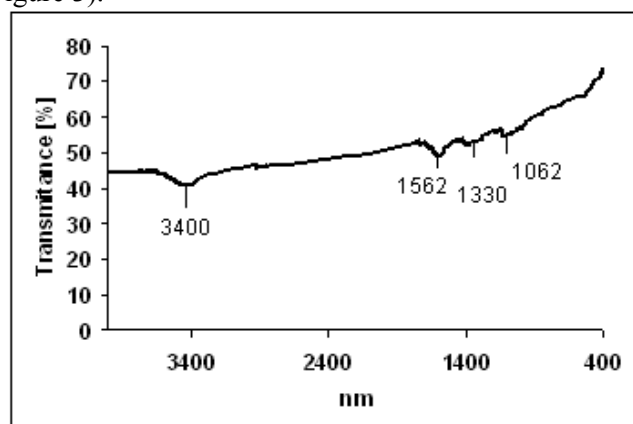


Fig. 3. FTIR spectrum of AuNPs-30

The first absorption at  $3410\text{cm}^{-1}$  is attributed to the stretching modes of vibration in hydroxyl functional group or NH stretching vibration in amines [30]. The two second absorption at approximately  $1560\text{ cm}^{-1}$  and  $1065\text{ cm}^{-1}$  correspond to a secondary amine NH band and primary amine CN stretch vibration of the proteins, respectively [31]. The other band at  $1350\text{ cm}^{-1}$  is assigned to CN stretching vibrations of aromatic amines [32]. It is well known that gold nanoparticles can be capped and stabilized by proteins through either free amine groups or cysteine residues in the protein and therefore stabilization of the gold nanoparticles by the surface-bound proteins is possible. Zeta potential measurements reveal the nanoparticles are highly stable and have an average surface charge of  $-26.77 \pm 0.7\text{ mV}$ . Evaluation of the zeta potential of the gold particles supports the stability of the nanoparticles indicated by the optical properties.

While bulk gold has been deemed “safe”, nanoscale particles of gold need to be examined for biocompatibility and environmental impact if they are to be manufactured on a large scale for various applications. The autofluorescence images of LoVo cancer cells are shown in Figure 4A. These strong autofluorescences are predominantly localized in the cells frame and will confuse the gold nanoparticles location. When the LoVo cancer cells were incubated in the presence of AuNPs-30 at the concentration of  $100\text{ }\mu\text{g/mL}$ , the cells grew at a normal rate. As can be seen from Figure 4B, the fluorescence signal are localized in spots in the cytoplasm. It seems that the cells incubated in the presence of AuNPs-30 exhibit stronger fluorescence and have more bright spots inside the cytoplasm that those without nanoparticles. The major problem was the interference of autofluorescence from cells under the same imaging condition. It is difficult to resolve which of these spots come from fluorescent particles due to the interference of autofluorescence from the cellular organelles. Despite this confusion, it seems that the biogenic gold nanoparticles can penetrate into LoVo cancer cells. There was a suspicion that these nanostructures were endocytosed by LoVo cells with evident bumps over the cell surface (Figure 4B). It is known that nanoparticles can be internalized by one or more of the following mechanisms: phagocytosis, pinocytosis, macropinocytosis and clathrin- and caveolin-mediated endocytosis. The electron microscopy technique (TEM) was used to confirm these assumptions.

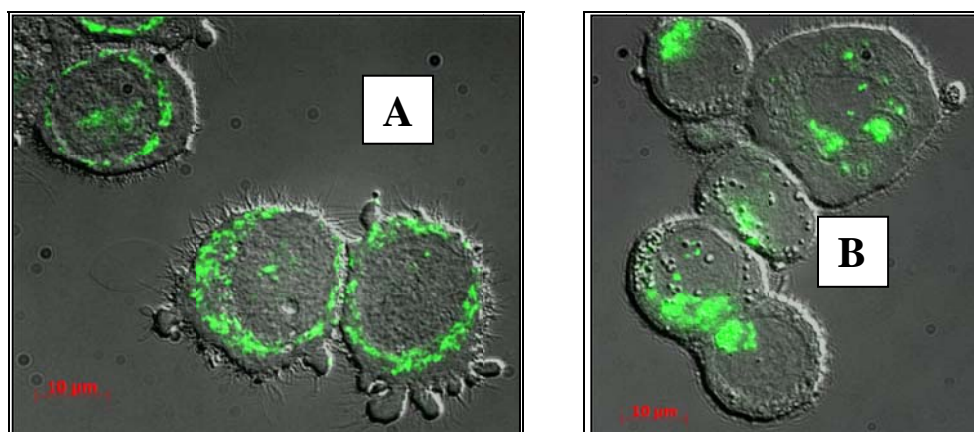


Fig. 4. Microscope images of: (A) LoVo cancer cells; (B) LoVo cancer cells incubated with AuNPs-30 after 24h.

Figure 5 panels A and B show TEM images of LoVo cancer cells incubated in medium containing AuNPs-30. As can be seen from Figure 5A, the nanoparticles are located in the extracellular region. After 24h of incubation, the gold nanoparticles were found in intracellular vesicles. Probably these vesicles contribute to the formation of endosomes and lysosomes, which are important acidic organelles. Moreover, it appears that some gold nanoparticles were capable of escaping from vesicles and were distributed in the cytoplasm (Fig. 5B). These results suggested that AuNPs-30 were taken up by LoVo cells via endocytosis. This is consistent with literature findings that in general, endocytosis is one of the important entry mechanisms for various

extracellular materials, particularly nanoparticles [33]. The mechanism of uptake can be dependent on many factors, such as, the physiochemical properties of gold nanoparticles (size and surface properties) and cell type. For example, Rejman et al. showed that the particles of sizes between 50 to 200 nm were taken up primarily by clathrin-mediated endocytosis, while particles of size 500 nm and above were taken up in a caveolin-dependent fashion [34]. Clathrin-mediated endocytosis occurs when gold nanoparticles accumulate on the cell membrane and clathrin-coated pits are formed to transport the NPs into the cell, resulting in the formation of endosomes.

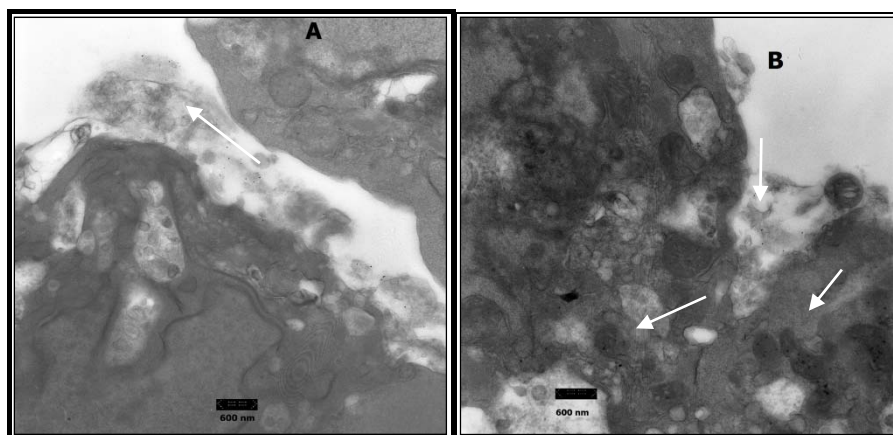


Fig. 5. TEM images of Lovo cancer cells incubated with AuNPs-30: (A) after 2h; (B) after 24h

The cytotoxic potential of CF, AuNPs and AuNPs-30 against human cancer cell line LoVo and sub-line LoVo/DX was examined using SRB method [23]. This well-known colorimetric assay estimates cell number indirectly by staining total cellular protein with the dye SRB (sulphorhodamine B is a bright pink aminoxanthine dye). In our study, the cells were treated with different concentrations of AuNPs, AuNPs-30 and CF for 72 hours. The proportions of surviving cells were then estimated and  $IC_{50}$  values (concentrations leading to 50% inhibition of viability) were calculated (Table 1). The data show that the cell-free filtrate strongly and specifically inhibited the proliferation of both cell lines (LoVo and Lovo/DX) with their  $IC_{50}$  values of

Table 1. Cytotoxicity of the cell-free filtrate and gold nanoparticles against colon cancer cell lines LoVo and LoVo/DX

	$IC_{50}$ [ $\mu\text{g/ml}$ ]	
	LoVo	LoVo/DX
CF <sup>1</sup>	14.15 $\pm$ 2.2	4.01 $\pm$ 1.7
AuNPs <sup>2</sup>	33.04 $\pm$ 4.9	28.88 $\pm$ 2.9
AuNPs-30 <sup>3</sup>	186.5 $\pm$ 7.3	146.0 $\pm$ 6.9

<sup>1</sup> The cell-free filtrate of *Trichoderma koningii*

<sup>2</sup> The gold nanoparticles synthesized by the cell-free filtrate of *Trichoderma koningii*

<sup>3</sup> The gold particles concentrated in the 30% sucrose fraction

14.15 $\pm$ 2.2  $\mu\text{g/mL}$  and 4.01 $\pm$ 1.7  $\mu\text{g/mL}$ , respectively, indicating the presence of cytotoxic compounds in the filtrate of *Trichoderma koningii*. In SRB assay, AuNPs were able to suppress proliferation of Lovo/DX cells more effectively than LoVo, with their  $IC_{50}$  values of 28.88 $\pm$ 2.9  $\mu\text{g/mL}$  and 33.04 $\pm$ 4.9  $\mu\text{g/mL}$ , respectively. Moreover, the results obtained reveal that AuNPs-30 have no significant cytotoxic effect on the cancer cells tested. Calculated values of  $IC_{50}$  are 186.5 $\pm$ 7.3  $\mu\text{g/mL}$  and 146.0 $\pm$ 6.9  $\mu\text{g/mL}$  against LoVo and LoVo/DX, respectively (Table 1). It was quantitatively confirmed that the filtrate protein in the gold nanoparticles synthesized by *Trichoderma koningii* is responsible for their noticeable cytotoxicity. These results strongly

highlight the importance of comparing the cell-free filtrate toxicity with the original nanoparticle solution as a precious control experiment to understand the origin of the nanoparticles toxicity.

### Conclusions

The results presented support the hypothesis that gold nanoparticles can be prepared and separated in a simple, eco-friendly and cost-effective manner. The simply sucrose density gradient technique to separate the gold nanoparticles based on their size could be successfully applied. Intracellular distribution of the smallest gold nanospheres has been studied with the general conclusion that these nanostructures are able to enter cancer LoVo cells and are trapped in vesicles, but are not able to enter the nucleus. Moreover, experimental results strongly indicate that the cell-free filtrate of *Trichoderma koningii* is responsible for the cytotoxicity of the gold nanoparticles against human cancer cell line LoVo and sub-line LoVo/DX. Even though these results may not accurately predict the *in vivo* toxicity it does provide a basis for understanding the mechanism of toxicity of nanoparticle uptake at the cellular level.

### Acknowledgement

This work was supported by NCN (grant no. NN 507 5150 58). I would like to thank Agnieszka Błażejczyk, MSc student for experimental assistance.

### References

- [1] K.S. Lee, M.A. El-Sayed, J. Phys. Chem. B. **110**, 19220, (2006).
- [2] M. Chakraborty, S. Jain, V. Rani, Appl. Biochem. Biotechnol. **165**, 1178, (2011).
- [3] E. Boisselier, D. Astruc, Chem. Soc. Rev. **38**, 1759, (2009).
- [4] X.M. Jiang, L.M. Wang, J. Wang, Ch.Y. Chen, Appl. Biochem. Biotechnol **166**, 1533, (2012).
- [5] K.B. Narayanan, N. Sakthivel, Adv. Coll. Inter. Sci. **156**, 1, (2010).
- [6] I. Maliszewska, in: Metal nanoparticles in microbiology (M. Rai, N. Duran, ed.), Springer-Verlag Berlin Heidelberg (2011).
- [7] M. Sastry, A. Ahmad, M.I. Khan, R. Kumar, Curr. Sci. **85**, 162, (2003).
- [8] A. Gade, A. Ingle, Ch. Whiteley, M. Rai, M. Biotechnol. Lett. **32**, 593, (2003).
- [9] M. Gericke, A. Pinches, Gold Bull. **39**, 22, (2006).
- [10] P. Mukherjee, S. Senapati, D. Mandal, A. Ahmad, M.I. Khan, R. Kumar, M. Sastry, ChemBioChem. **5**, 461, (2002).
- [11] S.S. Shankar, A. Ahmad, R. Pasricha, M. Sastry, J. Mat. Chem. **13**, 1822, (2003).
- [12] R. Sanghi, P. Verma, S. Puri, Adv. Chem. Eng. Sci. **1**, 154, (2011).
- [13] I. Maliszewska, Ł. Aniszkiewicz, Z. Sadowski, Acta Phys. Pol. A, **116**, 163, (2009).
- [14] R. Swarup, T. Mukherjee, S. Chakraborty, T. Kumar, Digest J. Nano. Biostruc. **8**, 197, (2013).
- [15] R. Bhambure, M. Bule, N. Shaligram, M. Kamat, R. Singhal, Chem. Eng. Technol. **32**, 1036, (2009).
- [16] R. M. Abd El- Aziz, M.R. Al-Othman, S.A. Al-Sohaibani, M. A. Mahmoud, S. R. M. Sayed, Digest J. Nano. Biostruc. **7**, 1491, (2012).
- [17] L. Du, L. Xian, J.X. Feng, J. Nanoparticles Res. **13**, 921, (2011).
- [18] J. Sarkar, S. Ray, D. Chattopadhyay, A. Laskar, K. Acharya, Bioprocess Biosyst. Eng. **35**, 637, (2012).
- [19] Y. Pan, S. Neuss, A. Leifert, M. Fischler, M., F. Wen, U. Simon, G. Schmid, W. Brandau, W. Jahnen-Dechent, Small, **3**, 1941, (2007).
- [20] C.M. Goodman, C. D. McCusker, T. Yilmaz, V.M. Rotello, Bioconjugate Chem. **15**, 897, (2004).
- [21] H.K. Patra, S. Banerjee, U. Chaudhuri, P. Lahiri, A.K. Dasgupta, Nanomedicine, **3**, 111, (2007).

- [22] S.A. Kumar, Y.A. Peter, J.L. Nadeau, *Nanotechnology*, **19**, 1, (2008).
- [23] S. Skehan, R. Storeng, D. Scudiero, A. Monks, J. McMahon, D. Vistica, J. T. Warren, H. Bokesch, S. Kenney, M.R. Boyd, *J. Nat. Cancer Inst.* **82**, 1107, (1990).
- [24] L.M. Liz-Marzan, *Mater. Today*, **7**, 26, (2004).
- [25] P. Mulvaney, *Langmuir*, **12**, 788, (1996).
- [26] F.K. Liu, G.T. Wei, *Anal. Chim. Acta*, **510**, 7, (2004).
- [27] M. Hanauer, S. Pierat, I. Zis, A. Lots, C. Sonnichsen, *Nano Letters*, **7**, 2881, (2007).
- [28] S.F. Sweeney, G.H. Woehrle, J.E. Hutchison, *J. Am. Chem. Soc.* **128**, 3190, (2006).
- [29] A. Henglein, *J. Phys. Chem.* **97**, 5457, (1993).
- [30] L. Castro, M.L. Blázquez, F. González, J.A. Muñoz, A. Ballester, *Chem. Eng. J.* **164**, 92, (2010).
- [31] V. Bansal, D. Rautaray, A. Bharde, K. Ahire, A. Sanyal, A. Ahmad, M. Sastry, *J. Mat. Chem.* **15**, 2583, (2005).
- [32] R. Sanghi, P. Verma, *Bioresource Technol.* **100**, 501, (2009).
- [33] A. Mukhopadhyay, Ch. Grabinski, A.R.M. Nabiul Afrooz, N.B. Saleh, S. Hussain, *Appl. Biochem. Biotechnol.* **167**, 327, (2012).
- [34] J. Rejman, V. Oberle, I.S. Zuhorn, D. Hoekstra, *Biochem. J.* **377**, 1, (2004).